MATERIALS RESEARCH COMMUNICATIONS
Vol. 1, No. 2 (2020) (12 pages)
@ Pusat Publikasi Ilmiah ITS

IMPACT BALLISTIC OF Cu-10wt%Sn FRANGIBLE BULLET BY EXPLICIT FINITE ELEMENT METHOD

KAMIL AKBAR E. AMARULLAH

Name of Department or Research Group,
Name of University or Laboratory,
Institution Address, Postcode, City, State/Province, Country
1st_author@mail.institution.domain

WIDYASTUTI

Department of Materials and Metallurgical Engineering,
Institut Teknologi Sepuluh Nopember,
Kampus ITS Keputih Sukolilo, 60111, Surabaya, East Java, Indonesia

MAS IRFAN P. HIDAYAT*

Department of Materials and Metallurgical Engineering,
Institut Teknologi Sepuluh Nopember,
Kampus ITS Keputih Sukolilo, 60111, Surabaya, East Java, Indonesia
irfan@mat-eng.its.ac.id

*** Corresponding author**

Received 31 December 2020

Abstract – In this work, impact ballistic of Cu-10wt%Sn frangible bullets is studied. The main objective of this study is to numerically investigate fragmentation and frangibility of the frangible bullet upon impacting a hard target. The fracture simulation is carried out using explicit finite element (FE) with element deletion/erosion technique to simulate the bullet-target interaction. The model employed maximum strain fracture criterion to model the bullet fracture. The applicability and capability of explicit FE model for simulating the bullet fracture are examined. Numerical results are validated against the experimental results.

Keywords: Impact ballistic; frangible bullet; explicit FE; frangibility; sintering.

1. Introduction

Many industrial components are produced by using powder metallurgy technique. By choosing process parameters properly such as compaction pressure, tooling dimensions, friction as well as sintering temperature, near-net products of single material or composite materials with good quality can be designed and produced. Powder metallurgy technique is also an easy and cheap manufacturing process so it has been a widely used manufacturing process. Due to such advantages and flexibilities, the technique is commonly employed to produce frangible bullets.

So far, micro-structural and mechanical behavior characterizations (Banovic, 2007; Mates et al., 2008) as well as microscopic fracture mechanisms (Banovic and Mates, 2008; Jian et al., 2013) of frangible bullets have been studied intensively. However, studies on frangibility of frangible bullets are only a few in literatures (Rydlo, 2010; Komenda et al., 2017; Bui et al., 2017). In particular, numerical investigation of impact ballistic and prediction of the bullet frangibility are still not explored intensively. In (Bui et al., 2017; Komenda et al., 2017), frangibility of frangible bullet upon impact on a hard target has been investigated experimentally, but intensive numerical study has not been carried out yet. The extension of such study would be a great interest and importance.

Commonly, investigations of impact ballistic concerned with hard projectile penetrating into plates made of steel, aluminum, concrete or brittle materials. For instances, ballistic penetration of steel plates has been investigated intensively in (Borvik et al., 1999; Borvik et al., 2002a; Borvik et al., 2002b). Liu et al. (2005)

presented structural intensity study of plates under low-velocity impact. Moreover, Polanco-Loria et al. (2008) performed numerical predictions of ballistic limits for concrete slabs using a modified concrete model. Finite element analysis with a nano-scale material model was carried out to study aluminium plates under impact loading (Johnsen et al., 2013). Mansur and Nganbe (2015) presented assessment of three finite element approaches for modeling the ballistic impact failure of metal plates. Numerical simulation of ballistic impact on armour plate with a simple plasticity model has been presented by Narayanamurthy et al. (2014). Yang et al. (2014) proposed an innovative procedure for estimating contact force during impact. In addition, studies of impacts on brittle materials have been investigated in (Michel et al., 2006; Zhu et al., 2018). Studies of impact on laminated composites have been also reported. Mohamadipoor et al. (2018) presented analytical and experimental investigation of ballistic impact on thin laminated composite plate. Transient response of a circular nanoplate subjected to low velocity impact has been studied by Liu et al. (2017), while elastic stress waves in an impacted plate was presented in (Liu et al., 2014). Bandaru and Ahmad (2015) studied effect of projectile geometry on the deformation behavior of kevlar composite armors under ballistic impact. Later on, responses of metal–ceramic functionally graded plates under low-velocity impact was also studied by Zu and Cai (2018). More recently, attentions have been also given to the impact loading on sandwich and foam structures as well as soft materials (Hedayatian et al., 2020; Elnasri and Zhao, 2020).

In other works, deformation and fracture modes of steel projectiles during impact have been studied as well in (Rakvag et al., 2013; Rakvag et al., 2014). It has been highlighted that it is necessary to have an accurate failure description for projectile material so that its fragmentation can be predicted well in a simulation for certain condition where the projectile may fracture or even fragment upon impact, and thus would not underestimate the ballistic limit velocity of the target plate. In regard to structure, property and behavior relationships, Holmen et al. (2013) examined effects of heat treatment on the ballistic properties of AA6070 aluminum alloy. In the paper, the ballistic properties of the aluminum alloy AA6070 in different tempers were studied, in which the tempers affected the alloy strength, strain hardening and ductility. In another study, effect of sintering temperature on the high strain rate-deformation of tungsten heavy alloys was studied by Hafizoglu and Durlu (2018). It was shown that an increase in the sintering temperature led to greater ductility, which in turn enhanced the plasticity and altered the fracture behavior of the alloy samples during Taylor impact testing.

Theoretical formulations for impact ballistic of frangible bullet allow theoretical prediction for the frangibility of frangible bullet, which is based upon the interaction analysis of frangible bullet and hard target (Rydlo, 2010; Komenda et al., 2017). On the other hand, numerical simulations may be used to display fracture debris of the bullet upon impact, while they can be related to the property and processing of materials as well. Nonetheless, the applicability and efficacy of various numerical models to simulate the fracture event need to be examined accordingly and compared with experimental observation and testing.

In this research work, impact ballistic of Cu-10wt%Sn frangible bullet is investigated and studied. The main objective of the present study is to numerically investigate fragmentation and frangibility of the frangible bullet upon impacting a hard target. Simulation of the bullet fracture upon impacting a cylindrical rigid target made of stainless steel is carried out using explicit FE method with element deletion/erosion technique to simulate the interaction between frangible bullet and target. Numerical results are presented and validated against the experimental results.

2. Modelling of Impact Ballistic of Frangible Bullet

2.1. *Impact Ballistic of Frangible Bullet*

From the terminal ballistics point of view, frangibility is the most important ballistic feature of frangible bullet. It is defined as the bullet capability to disintegrate into pieces upon hitting or impacting a hard target. Besides characteristics of frangible bullet and target, the interaction between frangible bullet and hard target also determines the disintegration/fragmentation events, thus the bullet frangibility. Theoretical prediction for the frangibility of frangible bullet can be obtained from the quasi-static analysis of frangible bullet and hard target interaction (Rydlo, 2010; Komenda et al., 2017).

In the analysis, some assumptions and simplifications are used, as follows:

(a) shape of frangible bullet is simplified as a cylinder and impacting a flat target

(b) bullet material is assumed to be homogeneous and isotropy, in particular with regard to small dimensions of frangible bullets
(c) bullet is modeled as an ideal elastic material, which is suitable for brittle material of frangible bullets based on a composite with metal matrix
(d) the character of load at axial compression test of frangible bullet materials is considered to be close to the one at the bullet impact on a hard target, and
(e) stress at any arbitrary section in the bullet due to the brake force is assumed to vary linearly from the tip of bullet to the bottom of bullet.

As the frangibility of frangible bullet is closely related to its kinetic energy limit $E_{K\lim}$, then it is important to get the value of its velocity limit $v_{\lim}$ in terms of properties of bullet and target and dimensions of bullet. By considering the Newton's third law of action-reaction, the brake force F_B acting against the motion of bullet equals the inertia force of bullet F_I caused by the deceleration of bullet:

$$F_B = F_I \tag{1}$$

$$c\delta = (\rho Sl)a \tag{2}$$

Here, c the stiffness of target, δ deformation of target, ρ bullet density, S transverse cross-section of bullet, l length of bullet and a deceleration of bullet due to the impact event.

Further, the variations of brake force F_B and stress σ_B due to the brake force at any cross-section at x distance measured from the bullet tip can be written as:

$$F_B(x) = \rho S(l-x)a \tag{3}$$

$$\sigma_B(x) = \rho(l-x)a \tag{4}$$

By using the ideal elastic material model, strain and deformation inside the bullet at any arbitrary position x can be defined respectively as:

$$\varepsilon_x(x) = \frac{\rho(l-x)a}{K} \tag{5}$$

$$u_x(x) = \int\left(\frac{1}{K}\rho(l-x)a\right)dx = \frac{\rho a}{K}\left(lx - \frac{x^2}{2}\right) + C \tag{6}$$

K is the modulus in compression and C is a constant, which can be obtained from the initial condition $u_{x,0}(0) = 0$, thus $C = 0$.

Moreover, the bullet relative compression $\varepsilon_{B\,rel}$ is taken as an average value given as:

$$\varepsilon_{B_{rel}} = \frac{\rho l a}{2K} \tag{7}$$

From (7), the maximum relative compression of bullet hence relates with the maximum deceleration of bullet $a_{\max}$:

$$\varepsilon_{B_{\max}} = \frac{\rho l a_{\max}}{2K} \tag{8}$$

Furthermore, by assuming that temperature rise due to the impact event is small, the conservation of energy between the kinetic energy E_K and the deformation works of bullet W_B and hard target W_C for the impact event at the moment right before the bullet will fracture can be written as:

$$E_K = W_B + W_C \tag{9}$$

$$\frac{m_B v_{\lim}{}^2}{2} = \frac{F_{B_{\max}}{}^2 l}{6KS} + \frac{F_{B_{\max}}{}^2}{2c} \tag{10}$$

$$v_{\lim}{}^2 = a_{\max}{}^2 \left(\frac{m_B l}{3KS} + \frac{m_B}{c} \right) \tag{11}$$

Solving for (11), it is finally obtained:

$$v_{\lim} = \frac{\varepsilon_{B_{\max}} 2K}{\rho l} \sqrt{m_B \left(\frac{4l}{3K\pi d_b{}^2} + \frac{1}{c} \right)} \tag{12}$$

2.2. *Mechanics of Solid Deformation and Fracture*

Time dependent deformation when a point initially at X_α moves to a point at x_i in a body can be expressed as follows (α = 1,2,3; i = 1,2,3) (Hallquist, 2006):

$$x_i = x_i(X_\alpha, t) \tag{13}$$

with initial conditions at time t = 0:

$$x_i(X_\alpha, 0) = X_\alpha \tag{14}$$

$$\dot{x}_i(X_\alpha, 0) = v_i(X_\alpha) \tag{15}$$

v_i defines the initial velocities.

Accordingly, the deformation gradient can be expressed as:

$$F_{ij} = \frac{\partial x_i}{\partial X_j} \tag{16}$$

Moreover, the following momentum equation needs to be resolved:

$$\sigma_{ij,j} + \rho f_i = \rho \ddot{x}_i \tag{17}$$

which satisfies the following traction, displacement and contact discontinuity boundary conditions along the boundaries ∂b_1, ∂b_2 and ∂b_3, respectively:

$$\sigma_{ij} n_i = t_i(t) \tag{18a}$$

$$x_i(X_\alpha, t) = D_i(t) \tag{18b}$$

$$\left(\sigma_{ij}{}^+ - \sigma_{ij}{}^- \right) n_i = 0 \tag{18c}$$

The equilibrium equation (17) can be also expressed as a statement of the principle of virtual work as follows (Hallquist, 2006):

$$\delta\pi = \int_{Vol} \rho \ddot{x}_i \delta x_i dV + \int_{Vol} \sigma_{ij} \delta x_{i,j} dV - \int_{Vol} \rho f_i \delta x_i dV - \int_{\delta b_1} t_i \delta x_i ds = 0 \tag{19}$$

where: σ_{ij} is the Cauchy stress, ρ the current density, f the body force, $\ddot{x}$ the acceleration, t_i the traction, Vol the volume, s the area/surface and ∂b_1 the unit outward normal to a boundary element of ∂b.

Further, the following energy equation is integrated in time and is used to update state condition and global energy balance:

$$\dot{E} = Vs_{ij}\dot{\varepsilon}_{ij} - (p+q)\dot{V} \tag{20}$$

in which s_{ij} and p respectively represent the deviatoric stresses and pressure:

$$s_{ij} = \sigma_{ij} + (p+q)\delta_{ij} \tag{21}$$

$$p = -\frac{1}{3}\sigma_{ij}\delta_{ij} - q = -\frac{1}{3}\sigma_{kk} - q \tag{22}$$

where: q is the bulk viscosity, δ_{ij} the Kronecker delta and $\dot{\varepsilon}_{ij}$ the strain rate tensor.

To define a fracture event, the following generic form of fracture criteria may be used (Johnson and Cook, 1985; Teng et al., 2007):

$$\int_0^{\bar{\varepsilon}_{pl}} F(\text{stress states}, \text{strain rates}, \text{temperature}, ...) d\bar{\varepsilon}_{pl} \geq D_c(\text{material}) \tag{23}$$

where: D_c is the critical damage index at the point of material fracture, $\bar{\varepsilon}_{pl}$ the effective plastic strain and σ_{ij} a general function of the variables of stress tensor, strain rate tensor, temperature or other variables. Considering the frangibility of frangible bullet in particular that is based upon metal matrix composite (Rydlo, 2010), a more straightforward fracture criterion can be used such as:

$$\bar{\varepsilon} \geq \varepsilon_f \tag{24}$$

where: ε_f is the strain at failure.

3. Materials and Methods

3.1. *Material properties and experiments*

Frangible bullets have been produced by a powder metallurgy technique with the variation of sintering temperatures. In addition, ballistic tests have been also carried out carefully for the purpose of experimental validation for this numerical study. A cylindrical steel plate with diameter of 800 mm and thickness of 20 mm, as shown in Fig. 1, was used as the hard target, where the targeted plate was placed in a bigger hollow cylinder to minimize the risk of bullet fragmentation. Table. 1 describes the bullets properties after sintering process and finishing, while the targeted plate properties are given in Table 2.

Fig. 2 depicts the bullet fragmentation after impacting the hard target. The representative fragments were produced from the frangible bullet processed with sintering temperature of 300 ^{0}C. The bullet fragments were shown to have different fragment sizes.

Attention has been also given to observe the bottom part fragments of the bullet upon impacting the hard target, as shown in Fig. 3.

Fig. 1. The cylindrical targeted plate.

Table 1. Properties of frangible bullets Cu-10%wtSn

Temperature (^{0}C)	Average mass (gr)	Density (gr/cm^3)	Young modulus (GPa)
200	6.122	7.700	54.38
300	6.114	7.711	57.28
400	6.113	7.683	61.27
500	6.121	7.696	67.16
600	6.165	7.767	76.60

Table 2. Mechanical properties of cylindrical targeted plate

Density (kg/m^3)	Yield strength (MPa)	Young modulus (GPa)	Poisson ratio
7850	250	200	0.26

Fig. 2. Representative fragments of frangible bullet Cu-10%wtSn.

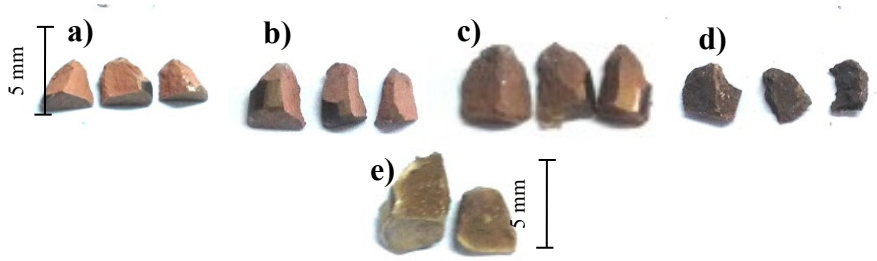

Fig. 3. Bottom part fragments of frangible bullets Cu-10%wtSn of different sintering temperatures: a) 200 ^{0}C, b) 300 ^{0}C, c) 400 ^{0}C, d) 500 ^{0}C and e) 600 ^{0}C, upon impact.

For numerical experiments, the values of modulus of elasticity with respect to the sintering temperatures shown in Table 1 are used as the inputted properties. To model the fracture and fragmentation of the bullet, fracture criterion of maximum strain is applied for both models. The bullet fragmentations from numerical simulations are then presented. Further, frangibility factor (*FF*) is evaluated accordingly by comparing the corresponding kinetic energy E_K to kinetic energy limit $E_{K\lim}$ having the bullet velocities after impact, given by:

$$FF = \frac{E_K}{E_{K\lim}} \tag{25}$$

The computations yield prediction of the bullet frangibility related to the material properties due to sintering temperature variations.

3.2. *Explicit FEM (LS-DYNA)*

Explicit FEM solves (19) by using mesh with FEM shape function and explicit time integration for marching in time. Moreover, contact algorithm is defined to model interaction between bullet and target. The contact algorithm may use penalty method, distributed parameter method and kinematic constraint method. In addition, whenever failure criterion is met, the explicit FEM will use erosion/deletion technique to remove the failed elements from computation. The applied load is then redistributed to the remaining surrounding elements. In this study, the explicit FEM is realized in LS-DYNA environment.

4. Results and Discussion

4.1. *Bullet erosion*

The element type of SOLID168 was used to mesh the bullet and target geometries. In addition, the bilinear kinematic plasticity material model was chosen for the frangible bullet, while the target was modelled as a rigid body. The bullet and target were discretized by using 6352 (9490 nodes) and 5857 elements, respectively. The initial velocity is set to be 345.2 m/s.

Fig. 4 shows the geometries and meshing of bullet and hard target before impact. Due to the deletion/erosion technique used in LS-DYNA, the failed elements were removed from computation, thus only remaining elements were shown.

In Fig. 5, the remaining parts of frangible bullets Cu-10%wtSn of different sintering temperatures upon impact are depicted. The LS-DYNA simulations show that not all elements or parts were eroded, thus emulating the remaining part of the bullet upon impacting the hard target i.e. the bullet bottom part. The results are in agreement with the experimental ballistic results shown in Figs. 2 and 3 that the largest fragment of the bullet upon the impact belongs to the bottom part.

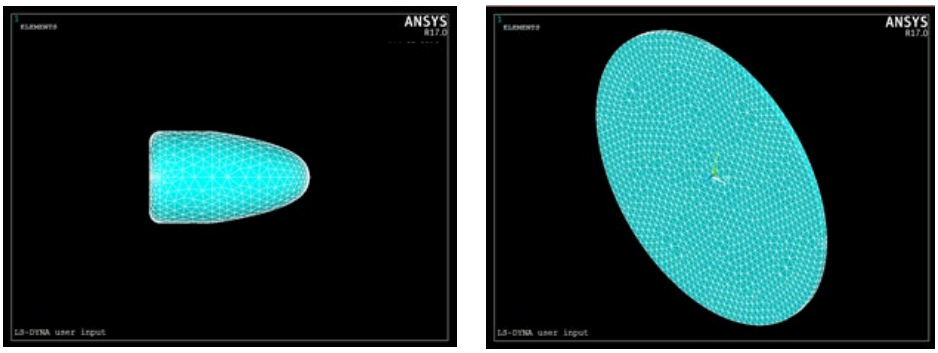

(a) (b)

Fig. 4. Geometries and meshing of: (a) bullet and (b) hard target in ANSYS LS-DYNA.

It is noted however that the explicit FEM cannot show the bullet fragmentation due to the deletion/erosion technique. This is the drawback in using the explicit FEM with deletion technique to model the fragmentation or debris of the frangible bullet. For clarity of presentation, the detailed erosion of the frangible bullet during the impact simulation is depicted in Fig. 6. It is shown between timeframes of 0.059 and 0.1 ms.

Note that the accuracies of the explicit FEM simulations presented above will be further verified with respect to the frangibility factor prediction, as discussed in the following section.

4.2. *Frangibility Prediction with The Explicit FEM*

Frangibility factor (FF) defines the frangibility of frangible bullet. Higher FF indicates that a frangible bullet will be easier to fragment upon impacting a hard target, which is preferred for the frangible bullet application. Referring to (25), the factor is related to the values of kinetic energy of bullet when impacting hard target and its kinetic energy limit. The $E_{K\lim}$ is defined as the lowest kinetic energy value at which the frangible bullet starts to break or fragment when impacting the hard target. Obviously, its value is closely related to the velocity limit $v_{\lim}$, which is influenced by the materials properties and geometries of frangible bullet and hard target, as shown in (12). The kinetic energy of bullet when impacting hard target can be obtained from numerical simulations.

Table 3 shows the prediction of FF values for the frangible bullets obtained from the explicit FEM simulations. Note that the velocities upon impact can be referred to Fig. 5. It is found that the accuracy of the explicit FEM model for predicting the bullet frangibility is about 15%, for the sintering temperature values between 200 ^{0}C and 500 ^{0}C. However, it appears that the present explicit FEM model fails for predicting the bullet frangibility at sintering temperature of 600 ^{0}C, as the predicted value of FF is less than one i.e. 0.94 showing that the bullet still did not produce any fracture.

From the view point of material property, the frangible bullet processed at sintering temperature of 600 ^{0}C posed higher ductility than bullets of other sintering temperatures. This fact is also reflected from the bullet frangibility factor, which is the lowest one. It seems that the bilinear kinematic plasticity material model in combination with maximum strain failure is less appropriate for modelling impact ballistic of frangible bullet, particularly for that with higher ductility.

In particular, the explicit FEM model produced lower values for the velocity of bullet upon impact than the expectation. This might be more impact energy has been absorbed by the bullet in the impact simulation. On the other hand, the fracture criterion has been met during the simulation. In addition, it might be also possible that

the conservation of energy during the impact simulation has been affected by the reduction of the bullet mass due to the eroded elements. As a result, the computed kinetic energy is underestimated.

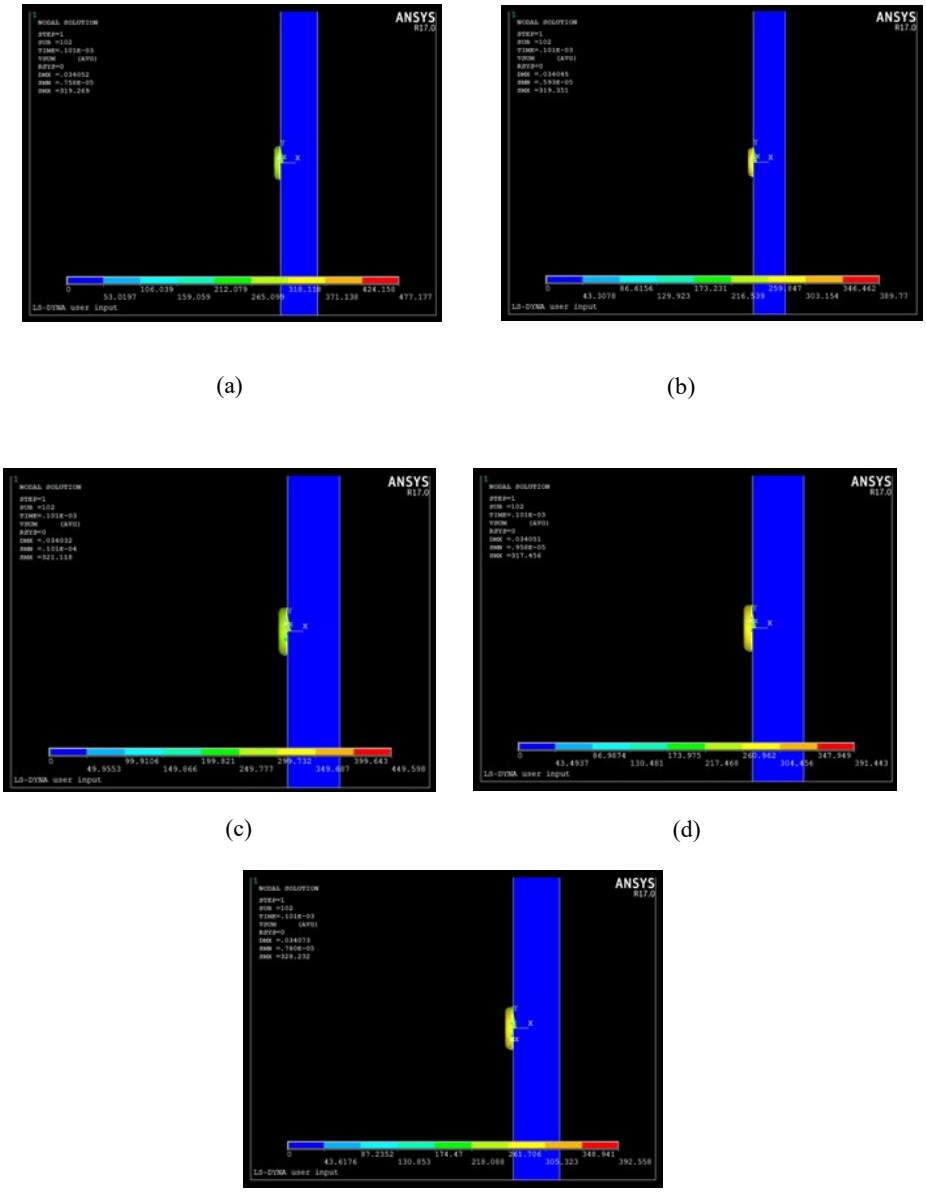

(a) (b)

(c) (d)

(e)

Fig. 5. The velocities and remaining part of frangible bullets Cu-10%wtSn of different sintering temperatures: (a) 200 ^{0}C, (b) 300 ^{0}C, (c) 400 ^{0}C, (d) 500 ^{0}C and (e) 600 ^{0}C, upon impact.

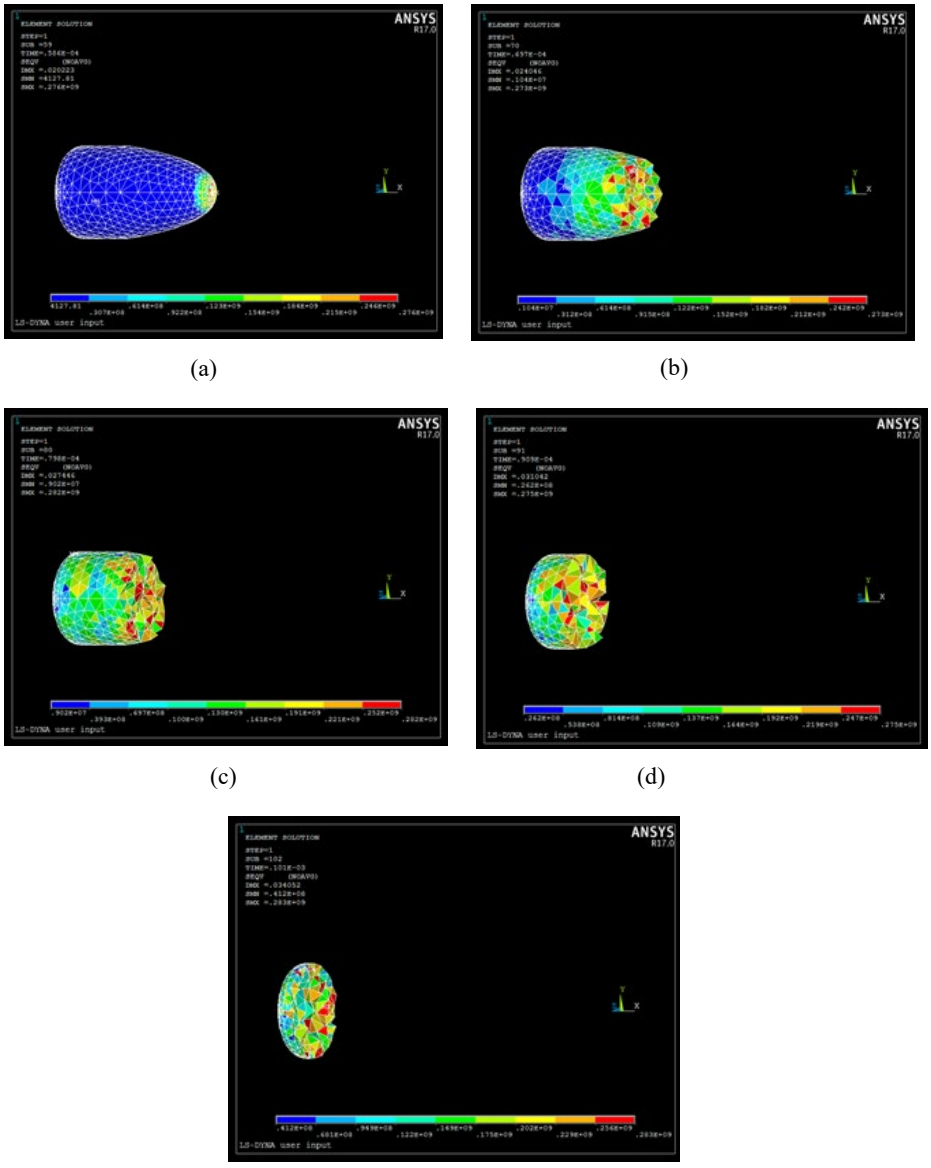

(a) (b)

(c) (d)

(e)

Fig. 6. Detailed erosion of the frangible bullet during the impact simulation in the explicit FEM model: (a) frame 1, (b) frame 2, (c) frame 3, (d) frame 4, and (e) frame 5.

Table 3. Prediction of FF values for the frangible bullets from the explicit FEM simulations

Sintering temperature (^{0}C)	Velocity of bullet upon impact (m/s)	KE (J) simulation	KE (J) experiment	FF simulation	FF experiment	FF prediction error (%)
200	319.27	312.02	368.79	7.90	9.34	15
300	319.35	311.77	368.34	5.71	6.74	15
400	321.12	315.18	368.21	3.67	4.29	14
500	317.46	308.44	368.73	1.91	2.28	16
600	328.23	332.09	371.31	0.94	1.05	-

The concern requires further investigation i.e. choice for more accurate material model combined with proper fracture criterion for modelling impact ballistic of frangible bullet by the explicit FEM. The model selection should give a good balance between evaluation of impact energy absorption and accurate initiation of fracture for frangible bullet. This may be subject for future study.

5. Conclusions

Investigation of impact ballistic of Cu-10wt%Sn frangible bullets by explicit finite element method has been presented in this study. The explicit model applicability for simulating the bullet fracture has been examined. The simulation results are validated against the experimental results. Numerical results showed that the explicit FE model can emulate remaining bottom part of the frangible bullet upon the impact. Nonetheless, the explicit FEM cannot show the bullet fragmentation due to the deletion/erosion technique. Choice for more accurate material model combined with proper fracture criterion for modelling impact ballistic of frangible bullet by the explicit FEM would be subject in future study.

References

Bandaru, A.K. and Ahmad, S. (2015) "Effect of Projectile Geometry on the Deformation Behavior of Kevlar Composite Armors Under Ballistic Impact," *International Journal of Applied Mechanics* **7**(3), 1550039-1 - 1550039-23.

Banovic, S. W. (2007) "Microstructural characterization and mechanical behavior of Cu-Sn frangible bullets," *Materials Science and Engineering A* **460-461**, 428–435.

Banovic, S. W. and Mates, S. P. (2008) "Microscopic fracture mechanisms observed on Cu-Sn frangible bullets under quasi-static and dynamic compression," *Journal of Materials Science* **43,** 4840-4848.

Borvik, T., Langseth, M., Hopperstad, O.S. and Malo, K.A. (1999) "Ballistic penetration of steel plates," *International Journal of Impact Engineering* **22**, 855-886.

Borvik, T., Langseth, M., Hopperstad, O.S. and Malo, K.A. (2002) "Perforation of 12mm thick steel plates by 20mm diameter projectiles with flat, hemispherical and conical noses Part I: Experimental study," *International Journal of Impact Engineering* **27**, 19-35.

Borvik, T., Langseth, M., Hopperstad, O.S. and Malo, K.A. (2002) "Perforation of 12mm thick steel plates by 20mm diameter projectiles with flat, hemispherical and conical noses Part II: numerical simulations," *International Journal of Impact Engineering* **27**, 37-64.

Bui, X.S., Komenda, J. and Vitek, R. (2017) "Frangibility of frangible bullet upon impact on a hard target," *Proc. of the International Conference on Military Technologies (ICMT)*, Brno, Czech Republic, pp. 7–11.

Buyuk, M., Kan, C.D.S. and Bedewi, N.E. (2008) "Moving Beyond the Finite Elements, a Comparison Between the Finite Element Methods and Meshless Methods for a Ballistic Impact Simulation," *Proc. of the Eighth International LS-DYNA Users Conference*, pp. 8-81 - 8-96.

Elnasri, I. and Zhao, H. (2020) "Impact Response of Sacrificial Cladding Structure with an Alporas Aluminum Foam Core Under Blast Loading," International Journal of Applied Mechanics 12(8), 2050094.

Hafizoglu, H. and Durlu, N. (2018) "Effect of sintering temperature on the high strain rate-deformation of tungsten heavy alloys," *International Journal of Impact Engineering* **121**, 44-54.

Hallquist, J.O. (2006) LS-DYNA Theory Manual. Livermore Software Technology Corporation (LSTC), Livermore.

Hedayatian, M., Daneshmehr, A. R. and Liaghat, G. H. (2020) "The Efficiency of Auxetic Cores in Sandwich Beams Subjected to Low-Velocity Impact," International Journal of Applied Mechanics 12(6), 2050061.

Holmen, J.K.., Johnsen, J., Jupp, S., Hopperstad, O.S. and Borvik, T. (2013) "Effects of heat treatment on the ballistic properties of AA6070 aluminium alloy," *International Journal of Impact Engineering* **57**, 119-133.

Jian, L., Ji-Li, R., Yu-Ning, Z., Tian-Fu, X. and Bin, L. (2013) "The material behaviour and fracture mechanisms of a frangible bullet composite," *Chinese Physics Letters* **30**(7)**,** 076202-1-076202-5.

Johnsen, J., Holmen, J.K.., Myhr, O.R., Hopperstad, O.S. and Borvik, T. (2013) "A nano-scale material model applied in finite element analysis of aluminium plates under impact loading," *Computational Materials Science* **79**, 724-735.

JOHNSON, G. R. and COOK, W.H. (1985) "FRACTURE CHARACTERISTICS OF THREE METALS SUBJECTED TO VARIOUS STRAINS, STRAIN RATES, TEMPERATURES AND PRESSURES," *Engineering Fracture Mechanics* **21**(1), 31-48.

Komenda, J., Bui, X.S., Vitek, R. and Jedlicka, L. (2017) "Evaluation method of frangible bullets frangibility," *Advances in Military Technology* **12**(2), 185-193.

Liu, J., Liu, H. and Yang, J.L. (2017) "Transient Response of a Circular Nanoplate Subjected to Low Velocity Impact," *International Journal of Applied Mechanics* **9**(8), 1750114-1 - 1750114-16.

LIU, Z., SUN, X. and GUO, Y. (2014) "ON ELASTIC STRESS WAVES IN AN IMPACTED PLATE," *International Journal of Applied Mechanics* **6**(4), 1450047-1 - 1450047-18.

Liu, Z.S., Lee, H.P. and Lu, C. (2005) "Structural intensity study of plates under low-velocity impact," *International Journal of Impact Engineering* **31**(8), 957-975.

Mansur, A. and Nganbe, M. (2015) "Assessment of three finite element approaches for modeling the ballistic impact failure of metal plates," *Journal of Materials Engineering and Performance* **24**(3), 1322-1331.

Mates, S. P., Rhorer, R., Banovic, S., Whitenton, E. and Fields, R. (2008) "Tensile strength measurements of frangible bullets," *International Journal of Impact Engineering* **35**, 511-520.

Michel, Y., Chevalier, J.-M., Durin, C., Espinosa, C., Malaise, F. and Barrau, J.-J. (2006) "Hypervelocity impacts on thin brittle targets: Experimental data and SPH simulations," *International Journal of Impact Engineering* **33**, 441-451.

Mohamadipoor, R., Zamani, E. and Pol, M.H. (2018) "Analytical and Experimental Investigation of Ballistic Impact on Thin Laminated Composite Plate," *International Journal of Applied Mechanics* **10**(2), 1850020-1 - 1850020-31.

Narayanamurthy, V., Rao, C.L. and Rao, B.N. (2014) "Numerical simulation of ballistic impact on armour plate with a simple plasticity model," *Defence Science Journal* **64**(1), 55-61.

Polanco-Loria, M., Hopperstad, O.S., Borvik, T. and Berstad, T. (2008) "Numerical predictions of ballistic limits for concrete slabs using a modified version of the HJC concrete model," *International Journal of Impact Engineering* **35**, 290-303.

Rakvag, K.G., Borvik, T. and Hopperstad, O.S. (2014) "A numerical study on the deformation and fracture modes of steel projectiles during Taylor bar impact tests," *International Journal of Solids and Structures* **51**, 808-821.

Rakvag, K.G., Borvik, T., Westermann, I. and Hopperstad, O.S. (2013) "An experimental study on the deformation and fracture modes of steel projectiles during impact," *Materials and Design* **51**, 242-256.

Rydlo, M. (2010) "Theoretical criterion for evaluation of the frangibility factor," *Advances in Military Technology* **5**(2), 57-67.

TENG, X., DEY, S. BØRVIK, T. and WIERZBICKI, T. (2007), "PROTECTION PERFORMANCE OF DOUBLE-LAYERED METAL SHIELDS AGAINST PROJECTILE IMPACT," *JOURNAL OF MECHANICS OF MATERIALS AND STRUCTURES* **2**(7), 1309-1330.

YANG, Y., SUN, J., LAM, N., ZHANG, L. and GAD, E. (2014) "AN INNOVATIVE PROCEDURE FOR ESTIMATING CONTACT FORCE DURING IMPACT," *International Journal of Applied Mechanics* **6**(6), 1450079-1 - 1450079-31.

Zhu, B. and Cai, Y. (2018) "Particle Size-Dependent Responses of Metal–Ceramic Functionally Graded Plates Under Low-Velocity Impact," *International Journal of Applied Mechanics* **10**(5), 1850056-1 - 1850056-21.

Zhu, Y., Liu, G.R., Wen, Y., Xu, C., Niu, W. and Wang, G. (2018) "Back-spalling process of an Al2O3 ceramic plate subjected to an impact of steel ball," *International Journal of Impact Engineering* **122**, 451-471.